1. Ionic polarizabilities as calculated from the present theory

Using experimental values of p_{44} and assuming the oscillator strength $f_1 = f_2 = 1$, we calculated the polarizabilities of the various ions for wavelength 5890 Å and compared them with the values obtained by other workers. The results are given in Table 2.

2. Polarizabilities of ions at different wavelengths

Equation (12) is used to calculate the polarizabilities of Cs^+ and I^- ions at different wavelengths in the range 3000–5890 Å. The data on the stress–optic dispersion are taken from Laiho & Korpela (1968) and refractive indices from Rodney (1955). The results are given in Table 3. The total polarizability is seen to increase towards shorter wavelength, while the polarizability of the positive ion is almost constant over the entire range.

Table 3. *Variation of polarizabilities of* Cs^+ *and* I^- *with wavelength*

Wavelength (Å)	α_{Cs}	α_I	$\alpha = \alpha_{Cs} + \alpha_I$
3022	2·56	8·56	11·12
3466	2·53	8·00	10·53
4047	2·52	7·59	10·11
4358	2·52	7·43	9·95
5085	2·52	7·27	9·79
5460	2·52	7·11	9·63
5790	2·52	7·06	9·58
5890	2·52	7·04	9·56

References

BANSIGIR, K. G. & IYENGAR, K. S. (1961*a*). *Acta Cryst.* **14**, 670–674.

BANSIGIR, K. G. & IYENGAR, K. S. (1961*b*). *Acta Cryst.* **14**, 727–732.

BORN, M. & HEISENBERG, W. (1924). *Z. Phys.* **23**, 388–410.

ETHIRAJ, R. & BANSIGIR, K. G. (1973). *Acta Cryst.* A**29**, 157–160.

ETHIRAJ, R., KRISHNA MURTY, V. G. & BANSIGIR, K. G. (1973). *Acta Cryst.* A**29**, 636–639.

FAJANS, K. & JOOS, G. (1924). *Z. Phys.* **23**, 1–46.

FRÖHLICH, H. (1949). *Theory of Dielectrics*. Oxford: Clarendon Press.

KITTEL, C. (1953). *Introduction to Solid State Physics*. New York: McGraw-Hill.

LAIHO, R. & KORPELA, A. (1968). *Ann. Acad. Sci. Fenn. A6*, pp. 272–276.

MUELLER, H. (1935). *Physics*, **6**, 179.

PAULING, L. (1927). *Proc. R. Soc. London*, A**114**, 191–199.

POCKELS, F. (1906). *Lehrbuch der Kristalloptik*. Berlin: Teubner.

RODNEY, W. (1955). *J. Opt. Soc. Am.* **45**, 987.

SHOCKLEY, W. (1946). *Phys. Rev.* **70**, 105.

Acta Cryst. (1978). A**34**, 321–326

Primary Extinction for Finite Crystals. Square-Section Parallelepiped

BY N. M. OLEKHNOVICH AND A. I. OLEKHNOVICH

Institute of Physics of Solids and Semiconductors, Byelorussian Academy of Sciences, Minsk 220726, *USSR*

(*Received* 14 *July* 1977; *accepted* 28 *October* 1977)

The results are given for the calculation of the profile function of the scattering curve and the calculated primary extinction factor for a crystal in the form of a square-section parallelepiped as a function of its size τ, expressed in extinction length units. The calculations are based on the equations of the dynamical theory of diffraction. Asymmetry of the scattering curve and a shift of its principal maximum to larger angles, with τ and the Bragg angle increasing, are found. Approximate expressions for calculating the primary extinction factor as a function of τ are given.

1. Introduction

As is shown, the existing approximations of the theory of X-ray diffraction in mosaic crystals are usually based on the supposition of primary and secondary extinction effects. The primary extinction is connected with the effect of coherent scattering in a single mosaic block. Being an incoherent effect of scattering, the secondary extinction is calculated by the Darwin–Zachariasen transfer equations. These equations have been used in estimating primary extinction in finite crystals (Zachariasen, 1967; Becker & Coppens, 1974), though they do not really apply to coherent scattering effects.

Primary extinction calculations, strictly speaking, should be based on the dynamical theory of diffraction, the solution of which for finite crystals of arbitrary configuration is a difficult problem. In the papers by Uragami (1969, 1970, 1971) and Afanas'ev & Kohn (1971) the method of solution of the equations of the Takagi–Taupin dynamical theory (Takagi, 1962, 1969; Taupin, 1967) for finite crystals has been developed. This method can be used for calculating the primary extinction factor and the angular distribution of X-ray intensity diffracted in a single mosaic block, which can be used for determining the scattering cross section per unit volume of a crystal, taking into account the effect of primary extinction in the transfer equations (Zachariasen, 1967; Becker & Coppens, 1974) as well as for establishing a connection between the primary and secondary extinction factors.

In this paper, on the basis of the Takagi (1969) equations, the results of calculating the angular distribution of intensity and the primary extinction factor for a crystal which is a square-section parallelepiped as a function of its size and its diffraction parameters are given.

2. Integral representation for the amplitude and power of diffracted radiation

The Takagi (1969) equations

$$\frac{\partial E_0}{\partial s_0} = -\frac{i\chi_0 K}{2}E_0 - \frac{i\chi_{-h}CK}{2}E_1$$

$$\frac{\partial E_1}{\partial s_1} = -i\left(\frac{\chi_0 K}{2} - \frac{\alpha K}{2}\right)E_1 - \frac{i\chi_h CK}{2}E_0, \quad (2.1)$$

determining the field amplitudes E_0 and E_1 in the crystal, can be written as

$$\frac{\partial^2 \mathscr{E}_{0,1}}{\partial s_0\,\partial s_1} + \sigma\mathscr{E}_{0,1} = 0 \quad (2.1a)$$

where

$$\mathscr{E}_{0,1} = E_{0,1}\exp[i\sigma_0(s_0 + s_1) - i\beta_1 s_1], \quad (2.2)$$

$$\sigma_0 = \frac{\chi_0 K}{2}; \quad \sigma = \sqrt{\sigma_1\sigma_2}; \quad \sigma_1 = \frac{\chi_{-h}CK}{2}; \quad \sigma_2 = \frac{\chi_h CK}{2};$$

$\beta_1 = \alpha K/2 = \varepsilon K \sin 2\theta_B$ and $\varepsilon = \theta_B - \theta$ is the angular divergence from the Bragg angle; χ_0, χ_{-h}, χ_h are the Fourier components of crystal polarizability for 0, $\bar{h}$ and h reciprocal lattice points respectively; K is the wave number; $C = 1$ or $\cos 2\theta_B$; s_0 and s_1 are coordinates of the real space along the incident and scattering vectors respectively.

The conventional integral form of representation of the solution of (2.1) (Uragami, 1969) can be reduced to

$$\oint U\frac{\partial V}{\partial s_0}\,ds_0 + V\frac{\partial U}{\partial s_1}\,ds_1 = 0$$

$$\oint V\frac{\partial U}{\partial s_0}\,ds_0 + U\frac{\partial V}{\partial s_1}\,ds_1 = 0, \quad (2.3)$$

where U is the amplitude of the field $\mathscr{E}_0$ or $\mathscr{E}_1$ and V is the Green's function fulfilling the conditions:

$$\left.\frac{\partial V}{\partial s_0}\right|_{s_1 = s_{1P}} = 0, \quad \left.\frac{\partial V}{\partial s_1}\right|_{s_0 = s_{0P}} = 0, \quad \left.V\right|_{\substack{s_0 = s_{0P}\\ s_1 = s_{1P}}} = 1. \quad (2.4)$$

s_{0P}, s_{1P} are coordinates of the point P at which the values of the field amplitudes are found.

We express the amplitude of the field of the radiation diffracted in a crystal having the form of square-section parallelepiped in integral form (Fig. 1). Our considerations are limited to the case of the Bragg angle in the range from 0 to 45°. The wave incident at s_0 on the crystal surface T_0R_0R has amplitude E_0^{in}. Depending on the boundary conditions of the Green's function, the contour R_0RT along which E_1 should be determined is divided into four parts: R_0R–RB_1–B_1B_2–B_2T.

When the integration contours (Fig. 1), which include R_0R, are considered the Green's function V_1^R fulfilling the condition $(\partial V_1^R/\partial s_0)|_{R_0R} = 0$ (Uragami, 1969) can be written as:

$$V_1^R = J_0\{2\sigma[(s_{0P} - s_0)(s_{1P} - s_1)]^{1/2}\} + \frac{\gamma_0\{[(s_{1P} - s_{1R_0})\gamma_1/\gamma_0] - s_0\}}{\gamma_1[s_{1R_0} + (s_{0P}\gamma_0/\gamma_1) - s_1]} \times J_2[2\sigma(\{[(s_{1P} - s_{1R_0})\gamma_1/\gamma_0] - s_0\} \times [s_{1R_0} + (s_{0P}\gamma_0/\gamma_1) - s_1])^{1/2}]. \quad (2.5)$$

On integration contours which include T_0T, the Green's function V_1^T fulfilling $V_1^T|_{T_0T} = 0$ is determined by

$$V_1^T = J_o\{2\sigma[(s_{0P} - s_0)(s_{1P} - s_1)]^{1/2}\} - J_0[2\sigma(\{s_{0T_0} + [s_{1P}\gamma_1/\gamma_0] - s_1\} \times \{[(s_{0P} - s_{0T_0})\gamma_0/\gamma_1] - s_1\})^{1/2}]. \quad (2.6)$$

On the contours which do not include either the upper

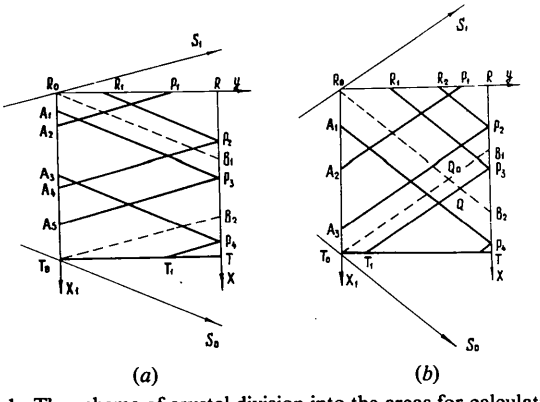

Fig. 1. The scheme of crystal division into the areas for calculation of the diffracted X-ray fields. (*a*) $0 \le \tan\theta_B \le 0{\cdot}5$, (*b*) $0{\cdot}5 \le \tan\theta_B \le 1$.

or the lower crystal boundary, the Green's function is determined by one term:

$$V_1 = J_0\{2\sigma[(s_{0P} - s_0)(s_{1P} - s_1)]^{1/2}\}. \quad (2.7)$$

Here J_0 and J_2 are the Bessel functions, $\gamma_{0,1} = |\cos(\mathbf{n}.\mathbf{s}_{0,1})|$, where $\mathbf{n}$ is vector of the inner normal to the surface R_0R or T_0T.

The case of diffraction when $0 \leq \tan\theta_B \leq 0{\cdot}5$

When (2.3) is applied to the contours $A_2P_1R_0A_2$, $A_4P_2R_1R_0A_4$, $A_5P_3A_1A_5$ and $T_1P_4A_3T_0T_1$, taking into account the corresponding boundary conditions we find amplitudes $\mathscr{E}_1$ on R_0R, RB_1, B_1B_2 and B_2T:

$$\mathscr{E}_{1P_1} = -i\sigma_2 \int_{R_0}^{P_1} \mathscr{E}_0^{\text{in}} V_1^R \, ds_1 - i\sigma_2 \int_{A_2}^{R_0} \mathscr{E}_0^{\text{in}} V_1^R \, ds_1, \quad (2.8)$$

$$\mathscr{E}_{1P_2} = -i\sigma_2 \int_{R_0}^{R_1} \mathscr{E}_0^{\text{in}} V_1^R \, ds_1 - i\sigma_2 \int_{A_4}^{R_0} \mathscr{E}_0^{\text{in}} V_1^R \, ds_1, \quad (2.9)$$

$$\mathscr{E}_{1P_3} = -i\sigma_2 \int_{A_5}^{A_1} \mathscr{E}_0^{\text{in}} V_1 \, ds_1, \quad (2.10)$$

$$\mathscr{E}_{1P_4} = -i\sigma_2 \int_{T_0}^{A_3} \mathscr{E}_0^{\text{in}} V_1^T \, ds_1, \quad (2.11)$$

where $\mathscr{E}_0^{\text{in}}$ is determined from E_0^{in} by (2.2). On passing to a rectangular coordinate system (Fig. 1) with $|\gamma_0| = |\gamma_1|$, we can write the expression for E_1, over the indicated ranges, as

$$E_{1P_1} = -\frac{i\sigma_2 t}{2\cos\theta_B} \exp\left[i\left(\frac{\kappa\tau}{\cos\theta_B} - \pi\beta\right)y\right] \times \left[\int_0^y E_0^{\text{in}}(y_1) D\,dy_1 + \int_0^y E_0^{\text{in}}(y_2) G\,dy_2\right], \quad (2.12)$$

$$E_{1P_2} = -\frac{i\sigma_2 t}{2\sin\theta_B} \exp\left[i\left(\frac{\kappa\tau}{\cos\theta_B} + \frac{\pi\beta x}{\tan\theta_B}\right)\right] \times \left[\int_x^{\tan\theta_B} E_0^{\text{in}}(x_2) L\,dx_2 + \int_0^{\tan\theta_B + x} E_0^{\text{in}}(x_1) M\,dx_1 + \int_0^{\tan\theta_B - x} E_0^{\text{in}}(x_1) N\,dx_1\right], \quad (2.13)$$

$$E_{1P_3} = -\frac{i\sigma_2 t}{2\sin\theta_B} \exp\left[i\left(\frac{\kappa\tau}{\cos\theta_B} + \frac{\pi\beta x}{\tan\theta_B}\right)\right] \times \int_{x-\tan\theta_B}^{x+\tan\theta_B} E_0^{\text{in}}(x_1) M\,dx_1, \quad (2.14)$$

$$E_{1P_4} = -\frac{i\sigma_2 t}{2\sin\theta_B} \exp\left[i\left(\frac{\kappa\tau}{\cos\theta_B} + \frac{\pi\beta x}{\tan\theta_B}\right)\right] \times \left[\int_{x-\tan\theta_B}^{1} E_0^{\text{in}}(x_1) M\,dx_1 - \int_{2-\tan\theta_B - x}^{1} E_0^{\text{in}}(x_1) T\,dx_1\right]. \quad (2.15)$$

Here

$$D = \exp\left[i\left(-\frac{\kappa\tau}{\cos\theta_B} + \pi\beta\right)y_1\right]\left\{J_0\left[\frac{\tau}{\cos\theta_B}(y - y_1)\right] + J_2\left[\frac{\tau}{\cos\theta_B}(y - y_1)\right]\right\}, \quad (2.16)$$

$$G = \exp[-i\pi\beta y_2]\left\{J_0\left[\frac{\tau}{\cos\theta_B}(y^2 - y_2^2)^{1/2}\right] + \frac{y - y_2}{y + y_2} J_2\left[\frac{\tau}{\cos\theta_B}(y^2 - y_2^2)^{1/2}\right]\right\}, \quad (2.17)$$

$$L = \exp\left\{i\left[\left(\frac{\kappa\tau}{\sin\theta_B} - \frac{\pi\beta}{\tan\theta_B}\right)x_2 - \frac{\kappa\tau}{\cos\theta_B}\right]\right\} \times \left\{J_0\left[\frac{\tau}{\sin\theta_B}(x_2^2 - x^2)^{1/2}\right] + \frac{x_2 - x}{x_2 + x} \times J_2\left[\frac{\tau}{\sin\theta_B}(x_2^2 - x^2)^{1/2}\right]\right\}, \quad (2.18)$$

$$M = \exp\left[-i\pi\beta\left(1 + \frac{x_1}{\tan\theta_B}\right)\right] \times J_0\left\{\frac{\tau}{\sin\theta_B}[\tan^2\theta_B - (x - x_1)^2]^{1/2}\right\}, \quad (2.19)$$

$$N = \exp\left[-i\pi\beta\left(1 + \frac{x_1}{\tan\theta_B}\right)\right] \times J_2\left\{\frac{\tau}{\sin\theta_B}[\tan^2\theta_B - (x + x_1)^2]^{1/2}\right\}, \quad (2.20)$$

$$T = \exp\left[-i\pi\beta\left(1 + \frac{x_1}{\tan\theta_B}\right)\right] \times J_0\left\{\frac{\tau}{\sin\theta_B}[\tan^2\theta_B - (2 - x - x_1)^2]^{1/2}\right\}, \quad (2.21)$$

$$\tau = \frac{r_0 C\lambda\sqrt{F_h F_{-h}}}{v} t, \quad \kappa = \frac{F_0}{C\sqrt{F_h F_{-h}}}, \quad \beta = -\frac{\beta_1 t}{2\pi\cos\theta_B},$$

$$y_2 = x_1\tan\theta_B; \quad x_2 = (1 - y_1)\tan\theta_B;$$

F_0, F_h, F_{-h} are structure amplitudes for reflections 0, h and $\bar{h}$; t is the edge length of the parallelepiped section; λ is the wavelength; v is the unit-cell volume.

The case of diffraction, when $0{\cdot}5 \leq \tan\theta_B \leq 1$

As can be seen from Fig. 1, in this case the amplitude E_1 on R_0R, RB_1 and B_2T will have the same form as that given above. To determine $\mathscr{E}_1$ in the area B_1B_2 (Fig. 1*b*) the expression (2.3) is applied to the contour $QP_3R_1R_0Q$ and, taking account of boundary conditions (2.4), one obtains

$$\mathscr{E}_{1P_3} = \mathscr{E}_{1O} - i\sigma_2 \int_{R_0}^{R_1} \mathscr{E}_0^{\text{in}} V_1^R \,\mathrm{d}s_1 - \int_{R_0}^{Q} \mathscr{E}_1 \frac{\partial V_1^R}{\partial s_0}\,\mathrm{d}s_0, \quad (2.22)$$

where $\mathscr{E}_1$ in the area R_0Q_0 is determined as was (2.10) and in the area Q_0Q as was (2.11).

Having made the necessary transformations in (2.22) and in passing to non-dimensional rectangular coordinate system with $|\gamma_0| = |\gamma_1|$, one obtains:

$$E_{1P_3} = -\frac{i\sigma_2 t}{2\sin\theta_B}\exp\left[i\left(-\frac{\kappa\tau}{\cos\theta_B} + \frac{\pi\beta x}{\tan\theta_B}\right)\right] \times \left[\int_x^{\tan\theta_B} E_0^{\text{in}}(x_2)\,L\,\mathrm{d}x_2 + \int_0^1 E_0^{\text{in}}(x_1)\,M\,\mathrm{d}x_1 + \int_0^{\tan\theta_B - x} E_0^{\text{in}}(x_1)\,N\,\mathrm{d}x_1 - \int_{2-\tan\theta_B - x}^1 E_0^{\text{in}}(x_1)\,T\,\mathrm{d}x_1\right]. \quad (2.23)$$

Then, from (2.12)–(2.15) and (2.23), the power and integrated intensity of scattering can easily be determined.

Integrated intensity can be represented by the following product:

$$\rho = \rho_k y_P \quad (2.24)$$

where ρ_k is the kinematical integrated intensity for the crystal and y_P is the primary extinction factor. The latter is determined by the integral:

$$y_P = \int_{-\infty}^{\infty} R(\beta)\,\mathrm{d}\beta. \quad (2.25)$$

Here $R(\beta)$ is a profile function of the scattering curve. With $\tan\theta_B \leq 0{\cdot}5$

$$R(\beta) = \frac{\tan\theta_B}{4\mathscr{P}_0}\int_0^1 J_y\,\mathrm{d}y + \frac{(\tan\theta_B)^{-2}}{4\mathscr{P}_0}\left[\int_0^{\tan\theta_B} J_{1x}\,\mathrm{d}x + \int_{\tan\theta_B}^{1-\tan\theta_B} J_{2x}\,\mathrm{d}x + \int_{1-\tan\theta_B}^1 J_{4x}\,\mathrm{d}x\right]; \quad (2.26)$$

with $0{\cdot}5 \leq \tan\theta_B \leq 1$

$$R(\beta) = \frac{\tan\theta_B}{4\mathscr{P}_0}\int_0^1 J_y\,\mathrm{d}y + \frac{(\tan\theta_B)^{-2}}{4\mathscr{P}_0}\left[\int_0^{1-\tan\theta_B} J_{1x}\,\mathrm{d}x + \int_{1-\tan\theta_B}^{\tan\theta_B} J_{3x}\,\mathrm{d}x + \int_{\tan\theta_B}^1 J_{4x}\,\mathrm{d}x\right], \quad (2.27)$$

where

$$J_y = \left|\int_0^y E_0^{\text{in}} D\,\mathrm{d}y_1 + \int_0^y E_0^{\text{in}} G\,\mathrm{d}y_2\right|^2,$$

$$J_{1x} = \left|\int_0^{\tan\theta_B} E_0^{\text{in}} L\,\mathrm{d}x_2 + \int_0^{\tan\theta_B + x} E_0^{\text{in}} M\,\mathrm{d}x_1 + \int_0^{\tan\theta_B - x} E_0^{\text{in}} N\,\mathrm{d}x_1\right|^2,$$

$$J_{2x} = \left|\int_{x-\tan\theta_B}^{x+\tan\theta_B} E_0^{\text{in}} M\,\mathrm{d}x_1\right|^2,$$

$$J_{4x} = \left|\int_{x-\tan\theta_B}^1 E_0^{\text{in}} M\,\mathrm{d}x_1 - \int_{2-\tan\theta_B - x}^1 E_0^{\text{in}} T\,\mathrm{d}x_1\right|^2,$$

$$J_{3x} = \left|\int_x^{\tan\theta_B} E_0^{\text{in}} L\,\mathrm{d}x_2 + \int_0^1 E_0^{\text{in}} M\,\mathrm{d}x_1 + \int_0^{\tan\theta_B - x} E_0^{\text{in}} N\,\mathrm{d}x_1 - \int_{2-\tan\theta_B - x}^1 E_0^{\text{in}} T\,\mathrm{d}x_1\right|^2,$$

and $\mathscr{P}_0$ is the power of the incident beam.

From (2.26) and (2.27) it follows that, if the cross section of the crystal is far less than the extinction length ($\tau \ll 1$), the function $R(\beta)$ with $\theta_B \leq 45°$ and $E_0^{\text{in}} = \text{const.}$ (plane incident wave) is

$$R(\beta) = \frac{\sin^2\pi\beta}{(\pi\beta)^2} + \frac{\tan\theta_B}{(\pi\beta)^2}\left[\cos^2\pi\beta - \frac{\sin 2\pi\beta}{2\pi\beta}\right]. \quad (2.28)$$

In this case

$$\int_{-\infty}^{\infty} R(\beta)\,\mathrm{d}\beta = 1.$$

The second term in (2.28) is stipulated by the edge effects.

3. Dependence of the profile function of the scattering curve and the primary extinction factor on crystal size

Using the above expressions, calculations of the $R(\beta)$ function and of the primary extinction factor y_p for the crystal form considered as a function of its size, τ, have been made using a program written in Fortran. The calculations were made for a plane incident wave and a non-absorbing crystal with different values of parameter κ.

From Fig. 2 it can be seen that as the crystal size increases the principal maximum decreases. In the chosen scale of measurements of the scattering angle β the integral half-width of the curve $R(\beta)$ increases with the size of crystal. This means that the integral half-

width of the scattering curve, with the effect of primary extinction taken into account, decreases more slowly with crystal size than in the kinematical case.

An effect of the κ parameter is revealed by the shift of the curve maximum $R(\beta)$ to larger scattering angles. This shift is caused by the so-called X-ray refraction effect. The calculation showed that the value of the curve-maximum shift $R(\beta)$ at a given Bragg angle and crystal size, τ, depends linearly on κ. At $\kappa = 0$ this maximum occurs with $\beta = 0$.

It is of interest to examine the dependence on the Bragg angle of the shift of the scattering curve maximum for a finite crystal of the form under investigation. With $\theta_B = 0$ in the symmetric crystal setting there is only the Laue diffraction for which, as is known, there is no X-ray refraction effect, *i.e.* at any κ value there is no shift of the reflecting curve maximum. When the Bragg angle is approaching 90°, only Bragg diffraction takes place, in which the maximum of the scattering curve is known to shift to larger angles by an amount $\chi_0/\sin 2\theta_B$. On the basis of our calculations we estimated the shift of the maximum of the scattering curve for different Bragg angles (Fig. 3). The shift ($\Delta\theta_m$) has been expressed in units of $\chi_0/\sin 2\theta_B$:

$$\Delta\theta_m \Big/ \frac{\chi_0}{\sin 2\theta_B} = \pi\beta_m \cos\theta_B/\kappa\tau.$$

Here β_m is the position of the maximum of $R(\beta)$ in units of β. As can be seen from Fig. 3 the shift of the maximum of the scattering curve for a finite crystal of the given form depends not only on the Bragg angle but also on the size of the crystal.

Fig. 4 shows the results of the calculation of the primary extinction factor for a finite crystal of the given form. From this figure it can be seen that when crystal size does not exceed the extinction length the primary extinction factor does not depend on the Bragg angle but when the size does exceed the extinction length the Bragg-angle values significantly affect the dependence of y_P on the size of the crystal.

In the case of Laue diffraction ($\theta_B = 0$) the primary extinction factor (y_P^0) as a function of the crystal size is affected by the known oscillation effect and is determined by the expression:

$$y_P^0 = \int_0^1 J_0^2[\tau(1-z^2)^{1/2}]\,dz, \qquad (3.1)$$

which is equivalent to the expression given by Zachariasen (1945, p. 133).

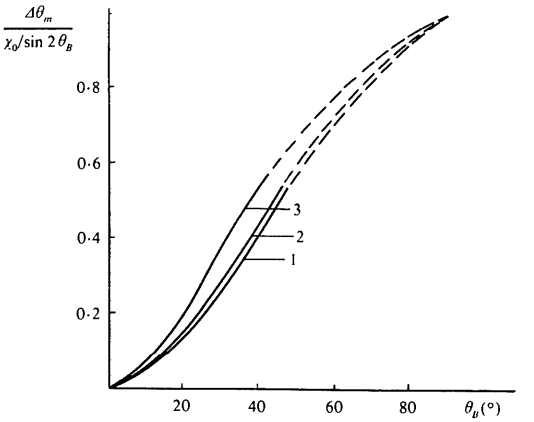

Fig. 3. Dependence on Bragg angle of the shift of the scattering curve maximum for a finite crystal with the form of a square-section parallelepiped. Solid line – calculations, dashed line – approximate interpolation: 1. $\tau = 0{\cdot}1$; 2. $\tau = 1$; 3. $\tau = 2$.

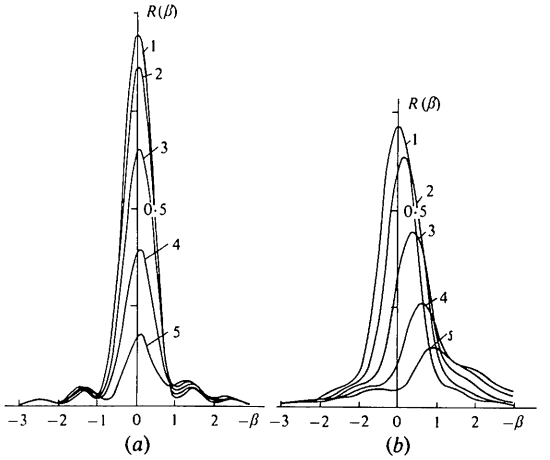

Fig. 2. The profile of the scattering curve for crystal blocks in the form of a square-section parallelepiped as a function of size: 1. $\tau \ll 1$; 2. $\tau = 0{\cdot}5$; 3. $\tau = 1{\cdot}0$; 4. $\tau = 1{\cdot}5$; 5. $\tau = 2{\cdot}0$; with $\kappa = 2$. (*a*) $\theta_B = 10°$, (*b*) $-\theta_B = 40°$.

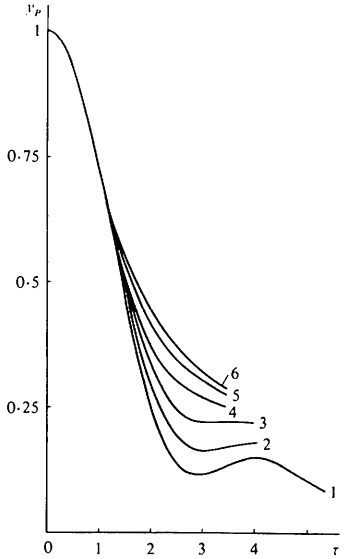

Fig. 4. Primary extinction factor *vs* the crystal size for different Bragg angles: 1. 0°; 2. 10°; 3. 20°; 4. 30°; 5. 40° and 6. 45°.

The analysis of the calculations carried out has shown that with $\tau \leq 3$, the value of the primary extinction factor can be determined with an error of 1·5% using the following approximate expressions:

$$y_P = y_P^0(1 - 2 \tan \theta_B) + y_P^1 2 \tan \theta_B \qquad (3.2)$$

with $0 \leq \tan \theta_B \leq 0{\cdot}5$ and

$$y_P = y_P^1 = \frac{\tanh \tau}{\tau} \{1 + 0{\cdot}445 \exp[-1{\cdot}64 \tan^3 \theta_B - 1{\cdot}09(\tau - 2{\cdot}6 \cos \theta_B)^2]\}^{-1} \qquad (3.3)$$

with $0{\cdot}5 \leq \tan \theta_B \leq 1$.

In the Bragg case the primary extinction factor for the square-section parallelepiped is greater than the factor for an infinite plate of the same thickness. This difference is greatest for small Bragg angles.

Conclusions

On the basis of X-ray dynamical diffraction theory the calculations of the primary extinction factor y_P and of the profile function of the scattering curve for a crystal block in the form of a square-section parallelepiped have been carried out. The calculations made it possible to determine the character of the variation of the scattering curve as a function of the size of the crystal, the zero Fourier coefficient of polarizability and the Bragg angle. It has been found that the primary extinction factor, when the crystal size does not exceed the extinction length ($\tau \leq 1$), does not depend on Bragg angle and is determined only by the size of the crystal. When $\tau > 1$ the relationship of primary extinction factor to τ is affected by the Bragg angle. When the Bragg angle is small, the factor y_P has oscillations which are caused by the Laue diffraction contribution. Approximate relationships for estimating the primary extinction factor have been found.

References

AFANAS'EV, A. M. & KOHN, V. G. (1971). *Acta Cryst.* A**27**, 421–430.

BECKER, P. J. & COPPENS, P. (1974). *Acta Cryst.* A**30**, 129–147.

TAKAGI, S. (1962). *Acta Cryst.* **15**, 1311–1312.

TAKAGI, S. (1969). *J. Phys. Soc. Jpn*, **26**, 1239–1253.

TAUPIN, D. (1967). *Acta Cryst.* **23**, 25–28.

URAGAMI, T. (1969). *J. Phys. Soc. Jpn*, **27**, 147–154.

URAGAMI, T. (1970). *J. Phys. Soc. Jpn*, **28**, 1508–1527.

URAGAMI, T. (1971). *J. Phys. Soc. Jpn*, **31**, 1141–1161.

ZACHARIASEN, W. H. (1967). *Acta Cryst.* **23**, 558–564.

ZACHARIASEN, W. H. (1945). *X-ray Diffraction in Crystals*. New York: John Wiley.

Acta Cryst. (1978). A**34**, 326–329

Self-Crystallizing Molecular Models. V. Molecular Charge Density Contours

BY TARO KIHARA AND KAZUO SAKAI

Department of Physics, Faculty of Science, University of Tokyo, Tokyo, Japan

(*Received* 12 *September* 1977; *accepted* 26 *October* 1977)

Molecular models with magnetic multipoles, which are used for simulating crystal structures, should resemble the actual molecules not only with respect to multipoles but also in shape. To obtain better knowledge of molecular shapes, charge-density contours have been calculated and illustrated for H_2, N_2, F_2, CO_2, C_2H_2, CH_4, CF_4, BF_3 and C_2H_4. The orthorhombic, low-temperature structure of solid acetylene established by Koski & Sándor [*Acta Cryst.* (1975), B**31**, 350–353], has been discussed on the basis of the molecular shape and the mechanism of phase transition from the cubic phase.

Introduction

The molecular models with magnetic multipoles, reported in this series of papers (Kihara, 1963, 1966, 1970, 1975), were invented for the purpose of explaining the crystal structures of nonpolar molecules.

If the molecules do not possess any appreciable electric multipoles, the crystal structures are governed by the condition of closest packing of the molecules.

If, on the other hand, the molecules have sufficiently strong electric multipoles, the electrostatic interaction often governs the crystal structure. This electrostatic multipolar interaction between molecules can be replaced by magnetic interaction between molecular models with magnetic multipoles. A structure into which these models are assembled will simulate the actual crystal structure.

The molecular model should resemble the actual